Microfluidics for 3D Cell and Tissue Cultures

Contributor: Gerardo Perozziello, Francesco Guzzi, Tania Limongi, Elvira Parrotta , Stefania Scalise, Valeria Lucchino, Francesco Gentile, Luca Tirinato, Bruno Torre, Marco Allione, Monica Marini, Francesca Susa, Enzo Di Fabrizio, Giovanni Cuda

Traditional cell cultures are performed in two-dimensional (2D) systems such as Petri dishes, multiwell plates or flasks. However, they cannot realistically mimic the morphophysiological complexity of the original three-dimensional (3D) in vivo environment from which the cells of specific lines originate. Without opposing animal experimentation but promoting its responsible application, the development of alternative cell culture systems tries to ensure compliance with the 3R principles. Reduction (reduction in the animals used for in vivo tests), Refinement (experimental design optimization to limit stress and affliction to laboratory animals) and Replacement (total or partial replacement of animal testing with alternative valid methods) are increasingly desired and strongly recommended as fundamental ethical aspects in the use of animals in scientific experiments.

1. Introduction

Traditional cell cultures are performed in two-dimensional (2D) systems such as Petri dishes, multiwell plates or flasks. However, they cannot realistically mimic the morphophysiological complexity of the original three-dimensional (3D) in vivo environment from which the cells of specific lines originate [1]. Without opposing animal experimentation but promoting its responsible application, the development of alternative cell culture systems tries to ensure compliance with the 3R principles. Reduction (reduction in the animals used for in vivo tests), Refinement (experimental design optimization to limit stress and affliction to laboratory animals) and Replacement (total or partial replacement of animal testing with alternative valid methods) are increasingly desired and strongly recommended as fundamental ethical aspects in the use of animals in scientific experiments [2].

Three-dimensional cell cultures can better mimic in vivo conditions than two-dimensional monolayer cell cultures, since, after isolation, cells generally lose their original morphology, changing the way they perform most of their physiological functions. Growth on an adhesion substrate results in cellular loss of polarity and it understandably influences intracellular trafficking, the functionality of subcellular compartments and some functions such as cell signaling and secretion, limiting the access to the culture media's nutrients, the gaseous exchanges and the removal of waste substances [3]. In 2D cell cultures the complex network of regulatory interactions in the extracellular matrix (ECM), cells and tissue are altered, therefore the use of properly designed 3D culture systems assists researchers in obtaining more reliable results, deepening our understanding of what really happens in vivo [4][5]. Many studies report data concerning the significant differences in the morphology, protein expression, differentiation, viability, and functionality of cells grown in 2D or 3D systems [1][3][6][7][8][9][10][11].

Three-dimensional cell cultures can be successfully used for many different applications, including cell or drug screenings [12][13][14][15] and tissue generation (engineering) purposes [16][17][18]; however, the reproduction of a biomimetic environment is challenging [19][20][21]. It is very important to replicate as close as possible the original in vivo physiological cell microenvironment. When dealing with 3D cell cultures, one of the big issues is to provide a physiological exchange of substances (gas and molecules) between cells and their related microenvironment, inward for the cell nutrients and outward for the waste products. It is known that unfortunately 2D cell culture usually results in low nutrients and/or hypoxic regions related to cellular aggregation phenomena, biological media and gas consumption rates [22].

The use of optimized ECM-analog biomaterials with physico-chemical and structural properties, able to guarantee optimized degradation or residence rate and micro/nanoporosity, improves in vitro cell proliferation, differentiation, and interactions [23][24].

Decellularized engineered ECM and bioreactor-based solutions constitute valid alternatives to 2D cell cultures. The application of decellularization protocols in tissue engineering and regenerative medicine limits the possible immune

response in the transplanted host by removing all the potential immunogenic biomaterials. The non-immunogenic ECM can be re-cellularized with autologous or stem cells, carrying out a fully personalized medicine approach [25][26]. In addition, micro-bioreactors can be regarded as a major step toward more complex organ-on-a-chip (OoC) systems [27], providing manageable 3D cell culture settings usually including suitable fluid flow supply and low amounts of chemicals and cells [28][29][30][31].

2. Physiological Exchange of Substances

In physiological conditions, the exchange of substances and gases between cells and the environment takes place thanks to blood microcirculation at the level of the capillaries. Blood circulates from the arterioles to capillaries, then to venules and the topology of these vessels changes according to the different tissues that are sprinkled. Some beds are structured as trees, others as arcades or sinuses or portal systems [32]. The capillary density (CD) depends on the varying oxygen and nutrients requirements to keep a stable metabolism. The average CD in human tissue is around 600 per mm^3 and it changes according to the different organism's tissues. The CD is higher in the brain, kidneys, liver and myocardium (around 2500–3000 per mm^3), reduced in the phasic units of the skeletal musculature (around 300–400 per mm^3) and even lower in the bones, fat, connective tissues and in the tonic units of the skeletal musculature (less than 100 per mm^3) [33].

Considering an average capillary diameter of 8 µm and length of 5 mm [34], it can be calculated the average distance between adjacent capillaries which is around 30–40 µm (around 1–3 cell width). To reach a particular cell, molecules exit the capillary and cross one or two cells to reach the target one. A capillary vessel can be considered as a tube consisting of a single endothelial cells' layer less than 1 µm thick [35]. There are three types of capillaries: (i) the continuous type with cells tightly joined together, which are present in muscles, nerves, and connective tissues; (ii) the fenestrated type, with cells so thin that internal vesicles form small pores 100 nm thick and 6 nm in diameter (typically around 1000 pores/μm^2); (iii) the discontinuous type with distinct intercellular gaps (around 5 µm in diameter) and a broken basement membrane, commonly found in organs such as the liver, spleen, and bone marrow, the functions of which include the injection or extraction of whole cells, large molecules and extraneous particles in/from the blood stream [36].

The nutritive and waste substances pass the capillary pores by means of a dynamic equilibrium established between the hydraulic pressure and the osmotic pressure gradients between the blood inside the capillaries and the interstitial fluid in the ECM. In particular, the blood's osmotic pressure (oncotic pressure) is around 25–30 mmHg and it is higher than the one of interstitial fluid which is around 0 mmHg. The osmotic pressure gradient is constant between the blood circuit and the surrounding tissues including the arterial capillaries and the venous capillaries. While the hydraulic pressure in blood decreases, going from the arterial capillaries (where it is around 40 mmHg) to the venous capillaries (which is around 15 mmHg), in the interstitial fluid it is around 2 mmHg. Since, in the arterial capillaries, the hydraulic pressure in the blood is higher than the oncotic pressure, filtration, a flow that goes from capillaries to tissues, occurs. On the contrary, in the venous capillaries, the oncotic pressure is higher than the hydraulic one and liquids are reabsorbed in capillaries due to a flow from tissues to capillaries (**Figure 1**).
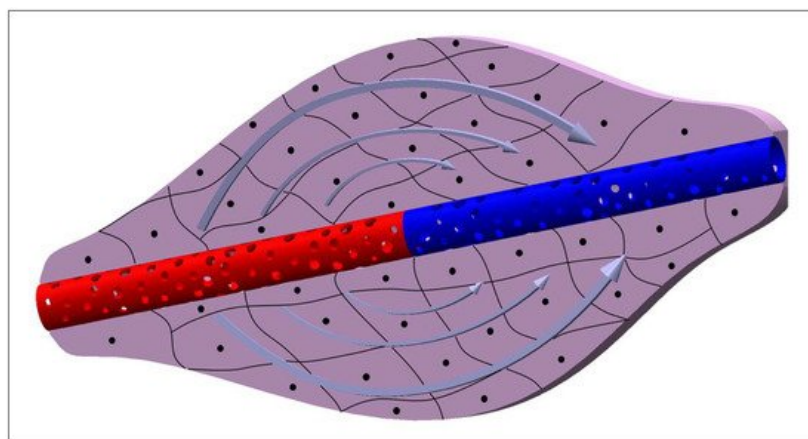
Figure 1. The scheme represents an arterial capillary (in red) connected to a venous capillary (in blue) and surrounded by a generic tissue constituted by cells. The arrows show the movement of fluids around the capillary, due to filtration (in the arterial side) and reabsorption (in the venous side).

The exchange of molecules between blood microcirculation and cells forming tissues and organs is due to filtration, reabsorption and at the same time diffusion through the capillary membrane of substances at a different concentration on

the two sides of the capillary membrane. The presence of capillaries drastically reduces the diffusion length, since they are very close to each other.

3. Theory behind the Molecule Transport Mechanisms

Referring to the theory behind the movement of particles across a capillary's membrane, it can be considered a unidimensional motion, assuming the concentration gradient across the membrane as constant. This approximation is certainly valid in the dynamic environment of the biological systems where, while cells consume nutrients and produce wastes, capillaries provide nutrients and remove wastes, keeping the concentration gradients across capillary's membrane constant.

The flux of molecules due to diffusion can be calculated as:

$$J_{dM} = -P\Delta C, \tag{1}$$

where

- $\Delta C = (C_2 - C_1)$ is the concentration gradient of a generic molecule between the external and internal part of the capillary membrane;
- P is the permeability coefficient and can be calculated as:

$$P = \frac{D_M \alpha}{\Delta x} = \frac{D_M n \pi R^2}{\Delta x}, \tag{2}$$

where

- Δx is the capillary membrane thickness;
- α is the partition coefficient and can be calculated as:

$$\alpha = \frac{N \pi R^2}{A} = n \pi R^2, \tag{3}$$

where

- N is the number of pores;
- A is the capillary surface;
- R is the pore radius;
- n is the pore density;
- D_M is the membrane diffusion coefficient and can be calculated as:

$$D_M = \epsilon D, \tag{4}$$

where

- ϵ is the hindrance coefficient and it depends on the particle and membrane pore dimension and the trajectory of the particle within the pore and can be calculated as:

$$\epsilon = \epsilon_1 \epsilon_2 = \left(1 - \frac{r}{R}\right)^2 \epsilon_2, \tag{5}$$

where

- ϵ_2 is a coefficient that depends on the trajectory of the particle inside the pore;
- r is the particle radius (it is an approximation which considers the molecules passing the pore to have a spherical shape);

- D is the diffusion coefficient which can be calculated as:

$$D = \frac{kT}{6\pi\eta r},$$

(6)

where

- k is the Boltzman constant;
- T is the temperature;
- η is the blood viscosity;

This last equation is valid if the particle which diffuses has a spherical shape. In this work, the particles will be considered, as first approximation, to have a spherical shape.

While the flux of molecules through the capillaries can be calculated as a function of the pressure and the osmotic gradient across the capillary.

$$J_{fM} = -\alpha \frac{C_1 + C_2}{2} \varepsilon L_p (\Delta p - \Delta \pi),$$

(7)

where

- $\Delta p = (p2 - p1)$ is the hydraulic pressure gradient across the capillary membrane;
- $\Delta \pi = (\pi2 - \pi1)$ is the osmotic pressure gradient across the capillary membrane;
- Lp is the filtration coefficient and can be calculated as:

$$L_p = \frac{n\pi R^4}{8\eta \Delta x},$$

(8)

For instance, considering a pore density of 100 pore/μm^2 [37], a pore diameter of 6 nm, a capillary thickness of 1000 nm, at a body temperature of 37 °C, a glucose molecule, with a relative radius of 4.5 Å and present at a concentration of 80 mg/dl in blood, will diffuse through the capillary at 28.5·10^{-2} mg/m^{2}s (roughly 7.6·10^{17} molecules/(m^{2}s)). In a capillary with 8 μm of diameter and 1 mm of length, there will be a flux of glucose due to the diffusion of 5.7·10^{-28} mg/s (roughly 1.5·10^{-9} molecules/s). In the same conditions, considering a pressure gradient of 40 mmHg and an osmotic pressure gradient of 25 mmHg, the flux of glucose due to filtration will be of 3.6·10^{-6} mg/m^{2}s (roughly 9.6·10^{12} molecules/m^{2}s). In a single capillary, the filtrated glucose will be 7.2·10^{-33} mg/s, corresponding to roughly 1.9·10^{-14} molecules/s. Thus, in the case of glucose, the dominant phenomenon is diffusion. Considering a total number of capillaries in the human body equal to 4·10^9, it can be calculated a movement of glucose equal to different kilograms per day. In general, the exchange of substances between blood and tissues is dominated by diffusion, referring to a very small space (as mentioned before: 2–3 cell width, around 40 μm).

## 4. Cell Microenvironment: Static and 3D Cell Screening

Mimicking the best possible cellular microenvironment does not only mean having control overflows, since many parameters such as shear stress, cell interactions, pH, CO_2, temperature, and O_2 variations affect its regulation and balance. Although it is well-known that in any kind of cell screening applications, it is very important to control the cell microenvironment, the current in vitro systems are still far from having an appreciable level of control on it [38]. Generally, supports such as Petri dishes, flasks and vials are used to culture cells in a static condition, leading to temperature and chemical gradients that could make it difficult to maintain homeostasis [39]. In addition, the use of standard static cell culture supports requires a lot of manual procedures, such as the addition of fresh culture medium and the removal of the old one, resulting in time-demanding procedures for the operator and stressful conditions for cells.

One of the alternatives to static cell culture procedures is the use of in vivo experiments that are undoubtedly able to reduce the gap between in vitro and in vivo screening procedures. Unfortunately, in vivo experimentation in basic and pre-clinical practice involves a considerable waste of resources, both in monetary and ethical terms, considering the number of animals to be sacrificed. Over the years and with the progress in biomedical and technological fields, there has been a

tendency to drastically reduce in vivo experiments using the advanced alternatives to animal testing towards the 3Rs (Replacement, Reduction, Refinement) approach. [40][41][42]. Although replacing should be the main purpose of the 3Rs, its implementation in the short-term is ambitious, while minimizing the number of animals and refining their welfare should be feasible in the short/middle-term [43].

A solid alternative to animal tests is cell scaffolds, as 3D cell culture can effectively mimic the cellular and tissue microarchitecture [44][45]. Both for pharmacological screening and pathologies modelling, 3D scaffolds represent one of the most successful platforms for biomedical applications [46][47][48][49].

Dattola et al. developed a poly(vinyl) alcohol (PVA) 3D scaffold where stem cells grew and differentiated into cardiac cells (**Figure 2**) [50]. These scaffolds mimicked the mechanical properties of ECM in which cardiomyocytes proliferated in vivo, demonstrated by the contractile property detected in the cardiomyocytes grown on the proposed scaffold. However, it was found that cells colonized only the outermost part of the scaffold, since they could not survive deep into the bulk volume, because the nutrients were not properly provided in the innermost layers of the 3D scaffolds.
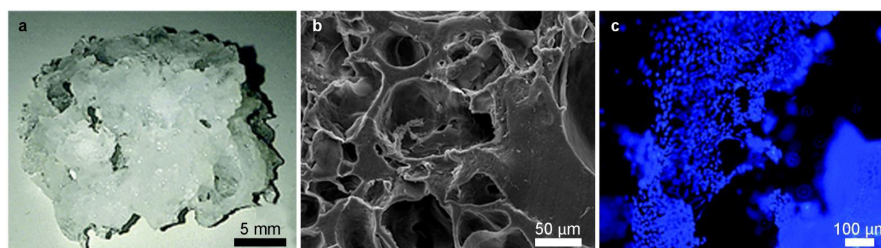
Figure 2. 3D PVA scaffolds in which stem cells are grown [50]. (**a**) macroscopic view of the 3D wet scaffold at room temperature; (**b**) scanning electron microscope cross sectional details of the 3D structure; (**c**) fluorescence microscopy image of DAPI stained cell homogeneously distributed on a Matrigel coated PVA scaffold.

They provided a continuous supply of nutrients and oxygen while removing metabolic wastes by creating an artificial network. This enabled the production of large, engineered tissues and the assembly of multiples organoids or spheroids to generate a whole system in vitro. Microfluidic systems also allowed precise culture conditions and better monitoring of cells. Once cells were cultured three-dimensionally in vitro, these considerations should be taken in account to reproduce in vivo conditions. In this contest microfluidic scaffolds effectively tried to solve the main issues related to the establishment of 3D cell cultures. Microfluidic systems, as an amelioration of the 3D scaffold methods, aimed to reduce in vitro cultured cells' discomfort and death related to inadequate nutrients distribution and catabolites clearance. Microfluidic cell culture solutions allowed non-invasively time-saving sampling and screening, reducing post-seeding inhomogeneity, since their tunable design and networks enable multiple and automated procedures [51].

Microfluidics assisted 3D cell culture by mechanically and chemically controlling cellular microenvironment, gas and temperature gradients, shear-stress and most of the relevant physical-chemical properties. Nowadays, these solutions are customized for the main biomedical applications, including cell therapy, drug, and toxicity assays (**Table 1**).

Table 1. Summary of a selection of the most representative and recent 3D microfluidic cell culture applications.

Microfluidic Platform Type	Application	Cell Lines	References
Resin 3D-printed system (VeroClear, MED610 resins)	**Cell Culture, LC-MS/MS single cell analysis**	**BPAECs (Bovine Pulmonary Artery Endothelial Cells), MDCK (Madin-Darby Canine Kidney)**	[52]
Microwell-based PDMS-membrane-PDMS sandwich multilayer chips	**Spheroid formation, OoC**	**C3A (liver)**	[53]
Two-stage temperature-controlling system used to generate decellularized extracellular matrix (dECM) hydrogel microspheres	**dECM hydrogels microsphere formation, cell culture**	**Schwann cells (nervous tissue), PC12 (adrenal gland)**	[54]
Injection-molded Polystyrene array	**OoC, angiogenesis**	**HUVEC (Human Umbilical Vein Endothelial Cells), fibroblasts**	[55]
PDMS-gut-on-a-chip device either with a straight channel or a non-linear convoluted channel, transwell-embedded hybrid chip	**OoC**	**Caco-2 (colon)**	[56]

Microfluidic Platform Type	Application	Cell Lines	References
Cyclo-olefin-polymer (COP) transparent bioreactor	On-chip platelet production	imMKCLs (immortalized MegaKaryocyte progenitor Cell Lines)	[57]
PDMS soft lithography replicas of superficial channels 3D-printed in different resins (Clear, Model, Tough, Amber, Dental resins)	OoC	HUVEC (Human Umbilical Vein Endothelial Cells), fibroblasts	[58]
PDMS bone-mimicking extracellular matrix composite device	Angiogenesis, OoC	SW620 (colon), MKN74 (stomach)	[59]
Single-chamber commercial microfluidic device	OoC, disease model, drug screening	Primary human hepatocytes, EA.hy926 (human endothelial), U937 (pleural effusion), LX-2 (hepatic stellate cell)	[60]
Collagen scaffold	OoC	Caco-2 (colon)	[61]
Cellulose-based device	Chemotaxis, invasion assay	A549 (lung)	[62]
Polymerized High Internal Phase Emulsion (polyHIPE) system	OoC	hES-MPs (human Embrionic Stem cell-derived Mesenchymal Progenitor cells)	[17]
OrganoPlate LiverTox™	Drug screening, OoC	Induced pluripotent stem cell (iPSC)-derived hepatocytes (iHep), endothelial cells, THP-1 monoblast (peripheral blood)	[63]
Injection-molded Polystyrene array	Drug screening	HeLa (uterus, cervix), NK-92 (peripheral blood)	[64]
Resin 3D-printed system (VeroClear)	Spheroid formation	OSCC (Oral Squamous Cell Carcinoma), HepG2 (liver)	[65]
3D-printed device	Circulating Tumour Cells (CTCs) isolation	MCF-7 (breast), SW480 (colon), PC3 (prostate), 293T (kidney)	[66]
PDMS-based device	Spheroid formation, disease model, drug screening, OoC	Rat primary hepatocytes, HSCs (Hepatic Stellate Cells)	[67]
PDMS-glass chip and Polycarbonate cover-plates	Four OoC	EpiIntestinal™, HepaRG (liver), HHStec (Human primary Hepatic Stellate cells), RPTEC/TERT-1 (human proximal tubule)	[68]
PDMS-based device	OoC	Hepatocytes from primary and iPS-derived cells	[69]
Three-layered glass device	OoC, disease model, drug screening	Primary human hepatocytes, LSECs (Liver Sinusoidal Endothelial Cells), Kupffer cells (liver)	[70]
Three-layered glass device	OoC, disease model, drug screening	Primary human hepatocytes, iPSC (induced-Pluripotent Stem Cells), endothelial cells, Kupffer cells (liver)	[71]
Silicon scaffold fabricated by deep reactive ion etching	OoC, disease model, drug screening	PHH (Primary Human Hepatocyte), non-parenchymal cells	[72]
PDMS "open-top" device	Angiogenesis, spheroid formation	HDMEC (Human Dermal Micro-vascular Endothelial Cells), Primary human lung fibroblasts, U87MG (nervous tissue)	[73]
PDMS based device	Angiogenesis, OoC	hLFs (human Lung Fibroblasts), HUVECs (Human Umbilical Vein Endothelial Cells)	[74]
Two-layered glass-PDMS hybrid system	Spheroid formation, invasion assay, drug screening	U87 (nervous tissue)	[75]
3D-printed system (Vero White Plus FullCure 835 resin)	Angiogenesis, cell culture, drug screening	bEnd.3 (mouse brain endothelial cell line)	[76]
Double-casting of PDMS, with master mold made of PMMA.	Spheroid formation, drug screening	Caco-2 (Colon), NHDF (Normal Human Dermal Fibroblast), HepG2 (liver), A549 (lung)	[77]

Microfluidic Platform Type	Application	Cell Lines	References
3D-hydrogel device	Drug screening, OoC	hCMEC/D3 (endothelial cell), HUVECs (Human Umbilical Vein Endothelial Cells), primary neurons, astrocytes	[78]
PDMS based device	OoC, drug screening	C3A (liver), EA.hy926 (endothelial)	[79]
PMMA-PDMS hybrid system and bioprinted hydrogel scaffold	OoC, angiogenesis	HUVECs (Human Umbilical Vein Endothelial Cells), neonatal rate cardiomyocytes	[80]
PDMS based device	OoC, disease model, drug screening	hiPSCs (human induced Pluripotent Stem Cells), CMs (Cardiomyocytes) differentiated from hiPSCs	[81]

Most of these studies concern drug screening and OoC applications, witnessing the increasing interest in regenerative and personalized medicine. Consulting the papers cited in the table, it is possible to extrapolate how, in general, microfluidics can reduce time and costs, allowing the implementation of high-throughput screening in drug discovery and disease models.

In the work of Shin et al. [56], a reproducible protocol to induce intestinal morphogenesis in microfluidic platforms using Caco-2 cell line was reported. Authors established a disease model, developing in vitro intestinal epithelial layers suitable to study intestinal physiology and host-microbiome interactions. Regional differentiation markers such as KRT20, villin, CEACAM1 and CYP3A4 were considerably expressed in the villus region, suggesting cytodifferentiation of the 3D epithelial layers.

Bircsak et al. [64] used an OrganoPlate LiverTox™ platform to co-culture three different cell lines: (i) iPSC-derived hepatocytes (ii) THP-1 monoblast and (iii) endothelial cells, respectively, in the ratio of 5:5:1, reproducing a hepatic model for hepatotoxicity. The liver model was evaluated for albumin, urea, alpha-fetoprotein synthesis, cell viability and CYP3A4 activity over 15 days. A total of 159 hepatotoxic compounds were screened, evaluating liver response to drugs using viability, nuclear size, urea and albumin assays.

In recent years, devices such as "body-on-a-chip" or "human-on-a-chip" have become ever more common and some of the recently proposed systems are already have the ability to reproduce multi-organ interactions. In Maschmeyer et al. [68], the authors introduced a four-organ-chip system modeling human intestine, liver, skin and kidney. The device, composed by two polycarbonate cover-plates and by a PDMS-glass chip, can accommodate both a blood and an excretory system, each controlled by a dedicated peristaltic micro-pump. This device has been designed to support absorption, distribution, metabolism and excretion (ADME) and profiling of substances, along with repeated toxicity testing of drugs. Authors successfully co-cultured the different cell types for 28 days, reporting a high cell viability and discrete physiological tissue architecture over the entire period. Finally, metabolic and gene analysis confirmed the establishment of a reproducible homeostasis between all four tissues.

References

1. Jensen, C.; Teng, Y. Is It Time to Start Transitioning From 2D to 3D Cell Culture? Front. Mol. Biosci. 2020, 7, 33.

2. Eder, C.; Falkner, E.; Nehrer, S.; Losert, U.M.; Schoeffl, H. Introducing the concept of the 3Rs into tissue engineering research. Altex 2006, 23, 17–23.

3. Kapałczyńska, M.; Kolenda, T.; Przybyła, W.; Zajączkowska, M.; Teresiak, A.; Filas, V.; Ibbs, M.; Bliźniak, R.; Łuczewski, Ł.; Lamperska, K. 2D and 3D cell cultures-a comparison of different types of cancer cell cultures. Arch. Med. Sci. 2018, 14, 910–919.

4. Ravi, M.; Paramesh, V.; Kaviya, S.R.; Anuradha, E.; Solomon, F.D. 3D cell culture systems: Advantages and applications. J. Cell. Physiol. 2015, 230, 16–26.

5. Li, X.J.; Valadez, A.V.; Zuo, P.; Nie, Z. Microfluidic 3D cell culture: Potential application for tissue-based bioassays. Bioanalysis 2012, 4, 1509–1525.

6. Toh, Y.C.; Lim, T.C.; Tai, D.; Xiao, G.; van Noort, D.; Yu, H. A microfluidic 3D hepatocyte chip for drug toxicity testing. Lab Chip 2009, 9, 2026–2035.

7. Carrion, B.; Huang, C.P.; Ghajar, C.M.; Kachgal, S.; Kniazeva, E.; Jeon, N.L.; Putnam, A.J. Recreating the perivascular niche ex vivo using a microfluidic approach. Biotechnol. Bioeng. 2010, 107, 1020–1028.

8. Cuchiara, M.P.; Allen, A.C.B.; Chen, T.M.; Miller, J.S.; West, J.L. Multilayer microfluidic PEGDA hydrogels. Biomaterials 2010, 31, 5491–5497.

9. Choi, J.; Kim, S.; Jung, J.; Lim, Y.; Kang, K.; Park, S.; Kang, S. Wnt5a-mediating neurogenesis of human adipose tissue-derived stem cells in a 3D microfluidic cell culture system. Biomaterials 2011, 32, 7013–7022.

10. Locatelli, L.; Inglebert, M.; Scrimieri, R.; Sinha, P.K.; Zuccotti, G.V.; Milani, P.; Bureau, L.; Misbah, C.; Maier, J.A.M. Human endothelial cells in high glucose: New clues from culture in 3D microfluidic chips. FASEB J. Off. Publ. Fed. Am. Soc. Exp. Biol. 2022, 36, e22137.

11. Jachter, S.L.; Simmons, W.P.; Estill, C.; Xu, J.; Bishop, C.V. Matrix-free three-dimensional culture of bovine secondary follicles to antral stage: Impact of media formulation and epidermal growth factor (EGF). Theriogenology 2022, 181, 89–94.

12. Langhans, S.A. Three-Dimensional in Vitro Cell Culture Models in Drug Discovery and Drug Repositioning. Front. Pharmacol. 2018, 9.

13. Wang, H.; Brown, P.C.; Chow, E.C.Y.; Ewart, L.; Ferguson, S.S.; Fitzpatrick, S.; Freedman, B.S.; Guo, G.L.; Hedrich, W.; Heyward, S.; et al. 3D cell culture models: Drug pharmacokinetics, safety assessment, and regulatory consideration. Clin. Transl. Sci. 2021, 14, 1659–1680.

14. Olgasi, C.; Cucci, A.; Follenzi, A. iPSC-Derived Liver Organoids: A Journey from Drug Screening, to Disease Modeling, Arriving to Regenerative Medicine. Int. J. Mol. Sci. 2020, 21, 6215.

15. Belfiore, L.; Aghaei, B.; Law, A.M.K.; Dobrowolski, J.C.; Raftery, L.J.; Tjandra, A.D.; Yee, C.; Piloni, A.; Volkerling, A.; Ferris, C.J.; et al. Generation and analysis of 3D cell culture models for drug discovery. Eur. J. Pharm. Sci. 2021, 163, 105876.

16. Bahrami, S.; Baheiraei, N.; Najafi-Ashtiani, M.; Nour, S.; Razavi, M. Chapter 9-Microfluidic devices in tissue engineering. In Biomedical Applications of Microfluidic Devices; Hamblin, M.R., Karimi, M., Eds.; Academic Press: Cambridge, MA, USA, 2021; pp. 209–233.

17. Bahmaee, H.; Owen, R.; Boyle, L.; Perrault, C.M.; Garcia-Granada, A.A.; Reilly, G.C.; Claeyssens, F. Design and Evaluation of an Osteogenesis-on-a-Chip Microfluidic Device Incorporating 3D Cell Culture. Front. Bioeng. Biotechnol. 2020, 8.

18. Choi, N.W.; Cabodi, M.; Held, B.; Gleghorn, J.P.; Bonassar, L.J.; Stroock, A.D. Microfluidic scaffolds for tissue engineering. Nat. Mater. 2007, 6, 908–915.

19. Wu, Q.; Liu, J.; Wang, X.; Feng, L.; Wu, J.; Zhu, X.; Wen, W.; Gong, X. Organ-on-a-chip: Recent breakthroughs and future prospects. BioMed. Eng. OnLine 2020, 19, 9.

20. van Duinen, V.; Trietsch, S.J.; Joore, J.; Vulto, P.; Hankemeier, T. Microfluidic 3D cell culture: From tools to tissue models. Curr. Opin. Biotechnol. 2015, 35, 118–126.

21. van Engeland, N.C.A.; Pollet, A.; den Toonder, J.M.J.; Bouten, C.V.C.; Stassen, O.; Sahlgren, C.M. A biomimetic microfluidic model to study signalling between endothelial and vascular smooth muscle cells under hemodynamic conditions. Lab Chip 2018, 18, 1607–1620.

22. Farhat, J.; Pandey, I.; AlWahsh, M. Transcending toward Advanced 3D-Cell Culture Modalities: A Review about an Emerging Paradigm in Translational Oncology. Cells 2021, 10, 1657.

23. Nii, T.; Makino, K.; Tabata, Y. Three-Dimensional Culture System of Cancer Cells Combined with Biomaterials for Drug Screening. Cancers 2020, 12, 2754.

24. Nii, T.; Makino, K.; Tabata, Y. A Cancer Invasion Model Combined with Cancer-Associated Fibroblasts Aggregates Incorporating Gelatin Hydrogel Microspheres Containing a p53 Inhibitor. Tissue Eng. Part C Methods 2019, 25, 711–720.

25. De Waele, J.; Reekmans, K.; Daans, J.; Goossens, H.; Berneman, Z.; Ponsaerts, P. 3D culture of murine neural stem cells on decellularized mouse brain sections. Biomaterials 2015, 41, 122–131.

26. Porzionato, A.; Stocco, E.; Barbon, S.; Grandi, F.; Macchi, V.; De Caro, R. Tissue-Engineered Grafts from Human Decellularized Extracellular Matrices: A Systematic Review and Future Perspectives. Int. J. Mol. Sci. 2018, 19, 4117.

27. Grün, C.; Altmann, B.; Gottwald, E. Advanced 3D Cell Culture Techniques in Micro-Bioreactors, Part I: A Systematic Analysis of the Literature Published between 2000 and 2020. Processes 2020, 8, 1656.

28. Manfredonia, C.; Muraro, M.G.; Hirt, C.; Mele, V.; Governa, V.; Papadimitropoulos, A.; Däster, S.; Soysal, S.D.; Droeser, R.A.; Mechera, R.; et al. Maintenance of Primary Human Colorectal Cancer Microenvironment Using a Perfusion Bioreactor-Based 3D Culture System. Adv. Biosyst. 2019, 3, e1800300.

29. Priyadarshini, B.M.; Dikshit, V.; Zhang, Y. 3D-printed Bioreactors for In Vitro Modeling and Analysis. Int. J. Bioprint. 2020, 6, 267.

30. Khan, I.; Prabhakar, A.; Delepine, C.; Tsang, H.; Pham, V.; Sur, M. A low-cost 3D printed microfluidic bioreactor and imaging chamber for live-organoid imaging. Biomicrofluidics 2021, 15, 024105.

31. Haycock, J.W. 3D cell culture: A review of current approaches and techniques. Methods Mol. Biol. 2011, 695, 1–15.

32. Myers, D.R.; Lam, W.A. Vascularized Microfluidics and Their Untapped Potential for Discovery in Diseases of the Microvasculature. Annu Rev. Biomed. Eng. 2021, 23, 407–432.

33. Freitas, R.A. Nanomedicine, Volume I: Basic Capabilities; Landes Bioscience: Georgetown, TX, USA, 1999; Volume 1.

34. Batra, S.; Rakusan, K. Capillary length, tortuosity, and spacing in rat myocardium during cardiac cycle. Am. J. Physiol. 1992, 263, H1369–H1376.

35. Alberts, B.; Johnson, A.; Lewis, J.; Raff, M.; Roberts, K.; Walter, P. Blood Vessels and Endothelial Cells. In Molecular Biology of the Cell, 4th ed.; Garland Science: New York, NY, USA, 2002.

36. Sarin, H. Physiologic upper limits of pore size of different blood capillary types and another perspective on the dual pore theory of microvascular permeability. J. Angiogenesis Res. 2010, 2, 14.

37. Bulger, R.E.; Eknoyan, G.; Purcell, D.J., 2nd; Dobyan, D.C. Endothelial characteristics of glomerular capillaries in normal, mercuric chloride-induced, and gentamicin-induced acute renal failure in the rat. J. Clin. Investig. 1983, 72, 128–141.

38. Tsai, H.F.; Trubelja, A.; Shen, A.Q.; Bao, G. Tumour-on-a-chip: Microfluidic models of tumour morphology, growth and microenvironment. J. R Soc. Interface 2017, 14, 20170137.

39. Enderle, J.D. Chapter 7-Compartmental Modeling. In Introduction to Biomedical Engineering, 3rd ed.; Enderle, J.D., Bronzino, J.D., Eds.; Academic Press: Boston, MA, USA, 2012; pp. 359–445.

40. Lipatov, V.A.; Kryukov, A.A.; Severinov, D.A.; Saakyan, A.R. Ethical and legal aspects of in vivo experimental biomedical research of the conduct. Part II. IP Pavlov Russ. Med. Biol. Her. 2019, 27, 245–257.

41. Baumans, V. Use of animals in experimental research: An ethical dilemma? Gene Ther. 2004, 11, S64–S66.

42. Mollaki, V. Ethical Challenges in Organoid Use. BioTech 2021, 10, 12.

43. Bédard, P.; Gauvin, S.; Ferland, K.; Caneparo, C.; Pellerin, È.; Chabaud, S.; Bolduc, S. Innovative Human Three-Dimensional Tissue-Engineered Models as an Alternative to Animal Testing. Bioengineering 2020, 7, 115.

44. Limongi, T.; Tirinato, L.; Pagliari, F.; Giugni, A.; Allione, M.; Perozziello, G.; Candeloro, P.; Di Fabrizio, E. Fabrication and Applications of Micro/Nanostructured Devices for Tissue Engineering. Nano-Micro Lett. 2016, 9, 1.

45. Limongi, T.; Cesca, F.; Gentile, F.; Marotta, R.; Ruffilli, R.; Barberis, A.; Dal Maschio, M.; Petrini, E.M.; Santoriello, S.; Benfenati, F.; et al. Nanostructured superhydrophobic substrates trigger the development of 3D neuronal networks. Small 2013, 9, 402–412.

46. Limongi, T.; Rocchi, A.; Cesca, F.; Tan, H.; Miele, E.; Giugni, A.; Orlando, M.; Perrone Donnorso, M.; Perozziello, G.; Benfenati, F.; et al. Delivery of Brain-Derived Neurotrophic Factor by 3D Biocompatible Polymeric Scaffolds for Neural Tissue Engineering and Neuronal Regeneration. Mol. Neurobiol. 2018, 55, 8788–8798.

47. Chaicharoenaudomrung, N.; Kunhorm, P.; Noisa, P. Three-dimensional cell culture systems as an in vitro platform for cancer and stem cell modeling. World J. Stem Cells 2019, 11, 1065–1083.

48. Gu, C.; Feng, J.; Waqas, A.; Deng, Y.; Zhang, Y.; Chen, W.; Long, J.; Huang, S.; Chen, L. Technological Advances of 3D Scaffold-Based Stem Cell/Exosome Therapy in Tissues and Organs. Front. Cell Dev. Biol. 2021, 9, 709204.

49. Zhang, L.; Yang, G.; Johnson, B.N.; Jia, X. Three-dimensional (3D) printed scaffold and material selection for bone repair. Acta Biomater. 2019, 84, 16–33.

50. Dattola, E.; Parrotta, E.I.; Scalise, S.; Perozziello, G.; Limongi, T.; Candeloro, P.; Coluccio, M.L.; Maletta, C.; Bruno, L.; De Angelis, M.T.; et al. Development of 3D PVA scaffolds for cardiac tissue engineering and cell screening applications. RSC Adv. 2019, 9, 4246–4257.

51. Tong, A.; Voronov, R. A Minireview of Microfluidic Scaffold Materials in Tissue Engineering. Front. Mol. Biosci. 2022, 8, 783268.

52. Currens, E.R.; Armbruster, M.R.; Castiaux, A.D.; Edwards, J.L.; Martin, R.S. Evaluation and optimization of PolyJet 3D-printed materials for cell culture studies. Anal. Bioanal Chem 2022, 414, 3329–3339.

53. Ma, L.-D.; Wang, Y.-T.; Wang, J.-R.; Wu, J.-L.; Meng, X.-S.; Hu, P.; Mu, X.; Liang, Q.-L.; Luo, G.-A. Design and fabrication of a liver-on-a-chip platform for convenient, highly efficient, and safe in situ perfusion culture of 3D hepatic spheroids. Lab Chip 2018, 18, 2547–2562.

54. Lin, Z.; Rao, Z.; Chen, J.; Chu, H.; Zhou, J.; Yang, L.; Quan, D.; Bai, Y. Bioactive Decellularized Extracellular Matrix Hydrogel Microspheres Fabricated Using a Temperature-Controlling Microfluidic System. ACS Biomater. Sci. Eng. 2022, 8, 1644–1655.

55. Yu, J.; Lee, S.; Song, J.; Lee, S.R.; Kim, S.; Choi, H.; Kang, H.; Hwang, Y.; Hong, Y.K.; Jeon, N.L. Perfusable micro-vascularized 3D tissue array for high-throughput vascular phenotypic screening. Nano Converg. 2022, 9, 16.

56. Shin, W.; Kim, H.J. 3D in vitro morphogenesis of human intestinal epithelium in a gut-on-a-chip or a hybrid chip with a cell culture insert. Nat. Protoc. 2022, 17, 910–939.

57. Kumon, H.; Sakuma, S.; Nakamura, S.; Maruyama, H.; Eto, K.; Arai, F. Microfluidic Bioreactor Made of Cyclo-Olefin Polymer for Observing On-Chip Platelet Production. Micromachines 2021, 12, 1253.

58. Carnero, B.; Bao-Varela, C.; Gómez-Varela, A.I.; Álvarez, E.; Flores-Arias, M.T. Microfluidic devices manufacturing with a stereolithographic printer for biological applications. Mater. Sci. Eng. C Mater. Biol. Appl. 2021, 129, 112388.

59. Ahn, J.; Lim, J.; Jusoh, N.; Lee, J.; Park, T.-E.; Kim, Y.; Kim, J.; Jeon, N.L. 3D Microfluidic Bone Tumor Microenvironment Comprised of Hydroxyapatite/Fibrin Composite. Front. Bioeng. Biotechnol. 2019, 7, 168.

60. Vernetti, L.A.; Senutovitch, N.; Boltz, R.; DeBiasio, R.; Shun, T.Y.; Gough, A.; Taylor, D.L. A human liver microphysiology platform for investigating physiology, drug safety, and disease models. Exp. Biol. Med. 2016, 241, 101–114.

61. Shim, K.Y.; Lee, D.; Han, J.; Nguyen, N.T.; Park, S.; Sung, J.H. Microfluidic gut-on-a-chip with three-dimensional villi structure. Biomed. Microdevices 2017, 19, 37.

62. Mosadegh, B.; Lockett, M.R.; Minn, K.T.; Simon, K.A.; Gilbert, K.; Hillier, S.; Newsome, D.; Li, H.; Hall, A.B.; Boucher, D.M.; et al. A paper-based invasion assay: Assessing chemotaxis of cancer cells in gradients of oxygen. Biomaterials 2015, 52, 262–271.

63. Bircsak, K.M.; DeBiasio, R.; Miedel, M.; Alsebahi, A.; Reddinger, R.; Saleh, A.; Shun, T.; Vernetti, L.A.; Gough, A. A 3D microfluidic liver model for high throughput compound toxicity screening in the OrganoPlate®. Toxicology 2021, 450, 152667.

64. Park, D.; Son, K.; Hwang, Y.; Ko, J.; Lee, Y.; Doh, J.; Jeon, N.L. High-Throughput Microfluidic 3D Cytotoxicity Assay for Cancer Immunotherapy (CACI-IMPACT Platform). Front. Immunol. 2019, 10, 1133.

65. Ong, L.J.Y.; Islam, A.; DasGupta, R.; Iyer, N.G.; Leo, H.L.; Toh, Y.C. A 3D printed microfluidic perfusion device for multicellular spheroid cultures. Biofabrication 2017, 9, 045005.

66. Chen, J.; Liu, C.Y.; Wang, X.; Sweet, E.; Liu, N.; Gong, X.; Lin, L. 3D printed microfluidic devices for circulating tumor cells (CTCs) isolation. Biosens. Bioelectron. 2020, 150, 111900.

67. Lee, J.; Choi, B.; No da, Y.; Lee, G.; Lee, S.R.; Oh, H.; Lee, S.H. A 3D alcoholic liver disease model on a chip. Integr. Biol. Quant. Biosci. Nano Macro 2016, 8, 302–308.

68. Maschmeyer, I.; Lorenz, A.K.; Schimek, K.; Hasenberg, T.; Ramme, A.P.; Hübner, J.; Lindner, M.; Drewell, C.; Bauer, S.; Thomas, A.; et al. A four-organ-chip for interconnected long-term co-culture of human intestine, liver, skin and kidney equivalents. Lab Chip 2015, 15, 2688–2699.

69. Schepers, A.; Li, C.; Chhabra, A.; Seney, B.T.; Bhatia, S. Engineering a perfusable 3D human liver platform from iPS cells. Lab Chip 2016, 16, 2644–2653.

70. Li, X.; George, S.M.; Vernetti, L.; Gough, A.H.; Taylor, D.L. A glass-based, continuously zonated and vascularized human liver acinus microphysiological system (vLAMPS) designed for experimental modeling of diseases and ADME/TOX. Lab Chip 2018, 18, 2614–2631.

71. Sakolish, C.; Reese, C.E.; Luo, Y.S.; Valdiviezo, A.; Schurdak, M.E.; Gough, A.; Taylor, D.L.; Chiu, W.A.; Vernetti, L.A.; Rusyn, I. Analysis of reproducibility and robustness of a human microfluidic four-cell liver acinus microphysiology system (LAMPS). Toxicology 2021, 448, 152651.

72. Ortega-Prieto, A.M.; Skelton, J.K.; Wai, S.N.; Large, E.; Lussignol, M.; Vizcay-Barrena, G.; Hughes, D.; Fleck, R.A.; Thursz, M.; Catanese, M.T.; et al. 3D microfluidic liver cultures as a physiological preclinical tool for hepatitis B virus infection. Nat. Commun. 2018, 9, 682.

73. Oh, S.; Ryu, H.; Tahk, D.; Ko, J.; Chung, Y.; Lee, H.K.; Lee, T.R.; Jeon, N.L. "Open-top" microfluidic device for in vitro three-dimensional capillary beds. Lab Chip 2017, 17, 3405–3414.

74. Nashimoto, Y.; Hayashi, T.; Kunita, I.; Nakamasu, A.; Torisawa, Y.-s.; Nakayama, M.; Takigawa-Imamura, H.; Kotera, H.; Nishiyama, K.; Miura, T.; et al. Integrating perfusable vascular networks with a three-dimensional tissue in a microfluidic device. Integr. Biol. 2017, 9, 506–518.

75. Ma, J.; Li, N.; Wang, Y.; Wang, L.; Wei, W.; Shen, L.; Sun, Y.; Jiao, Y.; Chen, W.; Liu, J. Engineered 3D tumour model for study of glioblastoma aggressiveness and drug evaluation on a detachably assembled microfluidic device. Biomed. Microdevices 2018, 20, 80.

76. Kim, J.A.; Kim, H.N.; Im, S.-K.; Chung, S.; Kang, J.Y.; Choi, N. Collagen-based brain microvasculature model in vitro using three-dimensional printed template. Biomicrofluidics 2015, 9, 024115.

77. Eilenberger, C.; Rothbauer, M.; Selinger, F.; Gerhartl, A.; Jordan, C.; Harasek, M.; Schädl, B.; Grillari, J.; Weghuber, J.; Neuhaus, W.; et al. A Microfluidic Multisize Spheroid Array for Multiparametric Screening of Anticancer Drugs and Blood–Brain Barrier Transport Properties. Adv. Sci. 2021, 8, 2004856.

78. Adriani, G.; Ma, D.; Pavesi, A.; Kamm, R.D.; Goh, E.L.K. A 3D neurovascular microfluidic model consisting of neurons, astrocytes and cerebral endothelial cells as a blood–brain barrier. Lab Chip 2017, 17, 448–459.

79. Jia, Z.; Cheng, Y.; Jiang, X.; Zhang, C.; Wang, G.; Xu, J.; Li, Y.; Peng, Q.; Gao, Y. 3D Culture System for Liver Tissue Mimicking Hepatic Plates for Improvement of Human Hepatocyte (C3A) Function and Polarity. BioMed Res. Int. 2020, 2020, 6354183.

80. Zhang, Y.S.; Arneri, A.; Bersini, S.; Shin, S.R.; Zhu, K.; Goli-Malekabadi, Z.; Aleman, J.; Colosi, C.; Busignani, F.; Dell'Erba, V.; et al. Bioprinting 3D microfibrous scaffolds for engineering endothelialized myocardium and heart-on-a-chip. Biomaterials 2016, 110, 45–59.

81. Veldhuizen, J.; Nikkhah, M. Developing 3D Organized Human Cardiac Tissue within a Microfluidic Platform. J. Vis. Exp. JoVE 2021.